Published OnlineFirst November 3, 2009; DOI: 10.1158/0008-5472.CAN-08-4673

Lin$^-$Sca-1$^+$CD49f^{high} Stem/Progenitors Are Tumor-Initiating Cells in the *Pten*-Null Prostate Cancer Model

David J. Mulholland,[1] Li Xin,[2] Ashkan Morim,[1] Devon Lawson,[2] Owen Witte,[1,2,3,4,5] and Hong Wu[1,4,5]

Departments of [1]Molecular and Medical Pharmacology and [2]Microbiology, Immunology and Molecular Genetics, [3]Howard Hughes Medical Institute, [4]Eli and Edythe Broad Center of Regenerative Medicine and Stem Cell Research, and [5]Institute for Molecular Medicine, University of California at Los Angeles, Los Angeles, California

Abstract

We have shown previously that *Pten* deletion leads to the expansion of subset of prostate cancer cells positive for CK5 and p63. Although this subpopulation may be involved in tumor initiation or progression, studies to date have not functionally validated this hypothesis. Using *in vitro* sphere-forming assay and *in vivo* prostate reconstitution assay, we show here the presence of a tumor-initiating subpopulation in the *Pten* prostate cancer mouse model. Specifically, we show that the Lin$^-$Sca-1$^+$CD49f^{high} (LSC) subpopulation overlaps with CK5$^+$; p63$^+$ cells and is significantly increased during prostate cancer initiation and progression and after castration. Mutant spheres mimic the structural organization of the epithelial compartment in the *Pten*-null primary tumor. Sorted LSC cells from either *Pten*-null spheres or primary tumors are able to regenerate prostate epithelial structure with cancerous morphology, closely mimicking that of primary cancers. Therefore, the LSC subpopulation is capable of initiating a cancerous phenotype that recapitulates the pathology seen in the primary lesions of the *Pten* mutant prostate model. [Cancer Res 2009;69(22):8555–62]

Introduction

Prostate cancer is the most common male malignancy and a leading cause of death in men in the western world (1). Although hormone ablation therapy is the typical mode of treatment for progressive disease, this therapy frequently fails when the disease advances to become castrate resistance. One theory accounting for the initiation and progression of prostate cancer as well as castration resistance is the presence of a rare subpopulation of transformed stem cells, often called cancer stem cells.

The presence of normal stem cells in the rodent prostate gland is well supported by androgen cycling experiments, resulting in continuous depletion and reconstitution of the prostatic epithelium (2, 3). The murine prostate epithelial compartment consists of p63/CD49/CK5$^+$ basal and CK8$^+$ luminal epithelial cells (4) as well as Syn/ChromA$^+$ neuroendocrine cells (5). These cell types differ in their proliferation/differentiation potentials and their response to androgen ablation.

Although the cytosolic markers are critical in identifying different cell types *in situ* in the prostatic epithelial compartment, the lack of cell surface markers for prospective cell isolation has hampered the identification and functional tests for stem/progenitor cells. Through a series of systematic studies, we and others have identified and validated the usefulness of markers such as stem cell antigen-1 (Sca-1; refs. 6, 7), CD49f (4, 6), CD117 (6), and Trop2 (8) for enriching murine stem/progenitor cell activity both *in vitro* in sphere-forming analysis and *in vivo* in prostate reconstitution assays. Sca-1$^+$CD49f^{high} enrichment, in conjunction with hematopoietic and endothelial lineage (CD45$^+$CD31$^+$Ter119$^+$) depletion, has lead to the identification of the Lin$^-$Sca-1$^+$CD49f^{high} (LSC) subpopulation. LSC and Lin$^-$Sca-1$^+$CD133$^+$CD44$^+$CD117$^+$ subpopulations are enriched in the proximal region of normal prostate and enhanced on androgen withdrawal (4, 6). Moreover, both subpopulations have been reported to contain sufficient progenitor activity for the regeneration of normal prostatic acini when grafted in conjunction with inductive urogenital mesenchyme (4, 6).

Although the aforementioned studies have identified cell surface markers for enriching stem/progenitor cells from the normal murine prostate, relatively few markers have been identified in the context of prostate cancer. Prostate cancer cell lines sorted for high expression of CD44 have been associated with enhanced expression of "stemness" markers including BMI, β-catenin, SMO, and Oct 3/4 (9). Moreover, CD44$^+\alpha_2\beta_1{}^+$CD133$^+$ subpopulations obtained from human tissue have enhanced capacity for *in vitro* serial passaging, although these subpopulations showed no correlation with tumor grade (10). CD133$^+$ has been used to identify subpopulations in hTERT immortalized human prostate epithelial cell lines with higher progenitor function (11). Recently, CD133$^+$ was shown to identify a minor population in human cell lines with stem-cell like qualities and the capacity to produce progeny with neuroendocrine, transit-amplifying, and intermediate cell characteristics (12).

Loss of PTEN is associated with prostate cancer initiation and metastasis (13). Previously, we have shown that prostate-specific deletion of *Pten* leads to invasive prostate cancer, mimicking many aspects of human disease (14). During prostate cancer progression, there is expansion of CK5$^+$, p63$^+$, and BCL2$^+$ cells in the proximal regions of the dorsolateral lobes (15), regions known to enrich in stem/progenitor activities in the normal prostate glands. We also showed that *Pten* deletion regulates basal cell proliferation and expansion (15). Collectively, these observations suggest that CK5$^+$;p63$^+$ subpopulation may associate with prostate cancer initiation and progression in the *Pten*-null prostate cancer model.

Our current study aims to identify the potential tumor-initiating cells in the *Pten*-null prostate cancer model. To do this, we have

Note: Supplementary data for this article are available at Cancer Research Online (http://cancerres.aacrjournals.org/).

Current address for L. Xin: Department of Molecular and Cell Biology, Baylor College of Medicine, Houston, TX 77030.

Requests for reprints: Hong Wu, Department of Molecular and Medical Pharmacology, Institute for Molecular Medicine, University of California at Los Angeles, CHS 23-214, 650 C.E. Young Drive South, Los Angeles, CA 90095-1735. Phone: 310-825-5160; Fax: 310-267-0242; E-mail: hwu@mednet.ucla.edu.

doi:10.1158/0008-5472.CAN-08-4673

Published OnlineFirst November 3, 2009; DOI: 10.1158/0008-5472.CAN-08-4673

taken a multipronged approach, including (*a*) *in vitro* sphere-forming analysis on sorted subpopulations for their stem/progenitor activities, (*b*) a sphere-mediated *in vivo* tissue reconstitution assay for their tumorigenic capacities, and (*c*) *in vivo* tissue regeneration assays, using the sorted subpopulations from primary cancers, to evaluate their tumor-initiating activities. Results derived from these complementary analyses are consistent and support the notion that the LSC subpopulation in the *Pten*-null prostate cancer model carries tumor-initiating activity.

Materials and Methods

Mouse strains, tissue collection, and reconstitution. Mutant mice with prostate-specific deletion of *Pten* were generated as described previously under a mixed background (14). To generate *ROSA26*^{LoxpSTOPLoxp}*-LacZ;Pb-Cre*$^{+}$*;Pten*$^{L/L}$ mice, *Pten* mutant mice were crossed to the *ROSA26*^{LoxpSTOPLoxp}*-LacZ* line (16). For clonality analysis, *Pb-Cre*$^{+}$*;Pten*$^{L/L}$ mice were crossed with either β-actin GFP [C57BL/6-TgN(ACTb-EGFP)1Osb] or β-actin dsRED [Tg (ACTB-DsRed.MST)1Nagy/J], purchased from The Jackson Laboratory. No obvious phenotype changes were detected on *Pten* conditional knockout mice when crossed to these reporter mice (data not shown). For *in vivo* reconstitution experiments, C57BL/6 female mice were used to obtain embryonic day 16/17 urogenital sinus mesenchyme (UGSM). Severe combined immunodeficient (SCID) mice were used for s.c. inoculations and prostate reconstitution and purchased from The Jackson Laboratory. Prostate tissue was harvested from 6- to 8-week-old donor mice and dissected to include all prostate lobes (including the proximal prostate infiltrating the urethra) but exclude the seminal vesicle and bladder as described previously (4, 17, 18). To remove gonadal androgens, surgical castrations were carried out on *Pb-Cre*$^{+}$*; Pten*$^{L/L}$ mice. All animal housing, breeding, and surgical procedures were done under the regulation of the Division of Laboratory Animal Medicine at the University of California at Los Angeles.

Prostate sphere assay. Prostate spheres were cultured and passaged as described previously (18).

Immunofluorescence and immunohistochemistry analyses. Tissue analysis was carried out using standard techniques as described previously (14). To stain prostate spheres, sphere cultures (Matrigel/sphere/prostate epithelial growth medium) were digested using 1 mg/mL dispase solution (Invitrogen) for 30 min at 37°C and subsequently incubated for 2 min with formalin. Spheres were washed in 70% ethanol and embedded in 20 to 30 μL histogel followed by standard paraffin processing and sectioning. For LacZ analysis, cultured spheres were treated with X-Gal solution for 4 to 6 h followed by fixation and embedding in histogel and paraffin. Areas positive for β-galactosidase activity stained blue. Sections of X-Gal–treated spheres were subsequently used for immunohistochemical analysis. CK5, CK8, p63, Ki-67, and CD49f immunodetection were carried out as described previously (4, 15).

Cytospin and staining. LSC^{+} and LSC^{-} subpopulations were separated by fluorescence-activated cell sorting (FACS) as described previously (4) and diluted to 5 × 10^{4}/mL and 100 μL diluted cells were cytospun onto glass slides using Cytospin3 (Shandon). Cells were then fixed with cold methanol, allowed to air dry, and stained using standard immunocytochemistry techniques.

FACS and analysis. Prostate lobes were digested in 1 mg/mL dispase solution (Invitrogen) for 30 min at 37°C and single-cell suspensions were stained with lineage markers (CD31, CD45, and Ter119), Sca-1, and CD49f as described previously (4). Cell sorting and analysis was done using the BD FACSvantage (BD Biosciences).

***In vivo* regeneration of prostate tissue.** UGSM was dissected and cultured as described previously (17, 19). For prostate regenerations from prostate spheres, 1 × 10^{5} UGSM cells were combined with 4 × 10^{3} sphere cells in 50% Matrigel/prostate epithelial growth medium and injected s.c. into a SCID mouse. For regenerations from primary prostate cells, 1 × 10^{5} UGSM cells were combined with 4 × 10^{3} LSC^{high}, LSC^{low}, or total unsorted cells in conjunction with or without total (Lin^{-}), control prostate epithelium. Grafts were harvested 6 to 8 weeks after injection.

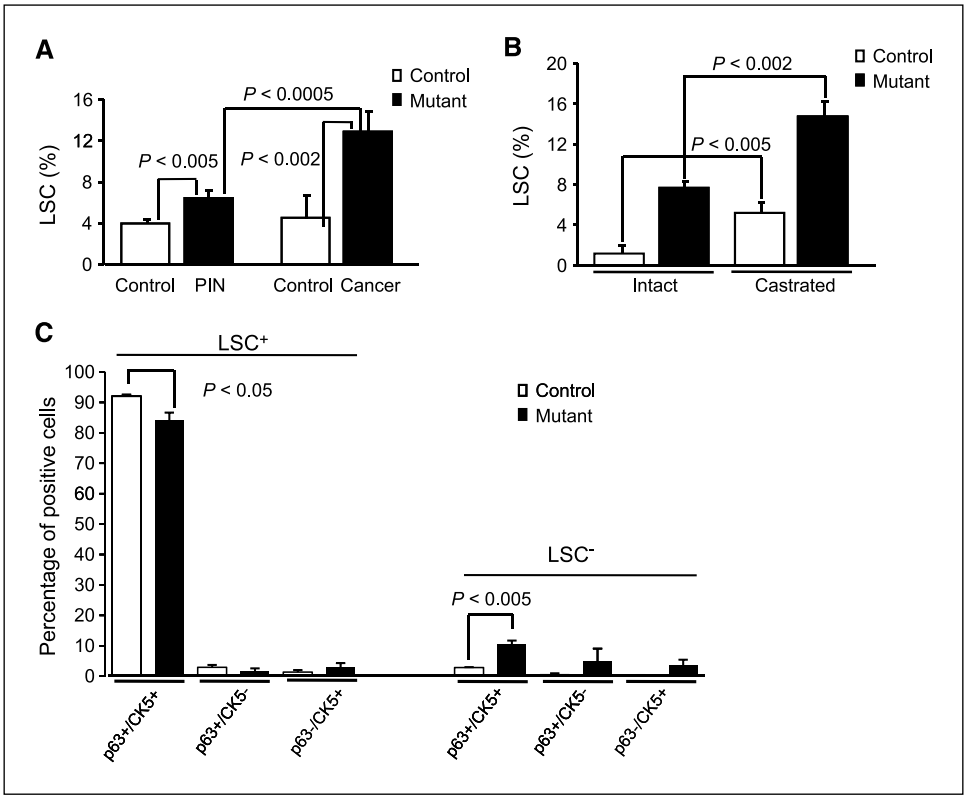

Figure 1. LSC content correlates with *Pten* mutant prostate cancer progression and is enhanced on androgen ablation. *A,* increased LSC^{+} subpopulation during prostate cancer initiation (*PIN*; 7 wk) and progression (*Cancer*, 20 wk) in *Pten* mutant prostate (n = 3) compared with controls (n = 3). *B,* castration enhances the percentage LSC^{+} cells in *Pten* mutants (n = 3) relative to intact mutants (n = 3) at 10 wk. This trend is also observed in control mice; however, the absolute LSC content is significantly lower than mutant mice. *C,* majority of mutant and control LSC^{+} cells are positive for the basal cell markers p63 and CK5 (p63^{+}/CK5^{+}).

Published OnlineFirst November 3, 2009; DOI: 10.1158/0008-5472.CAN-08-4673

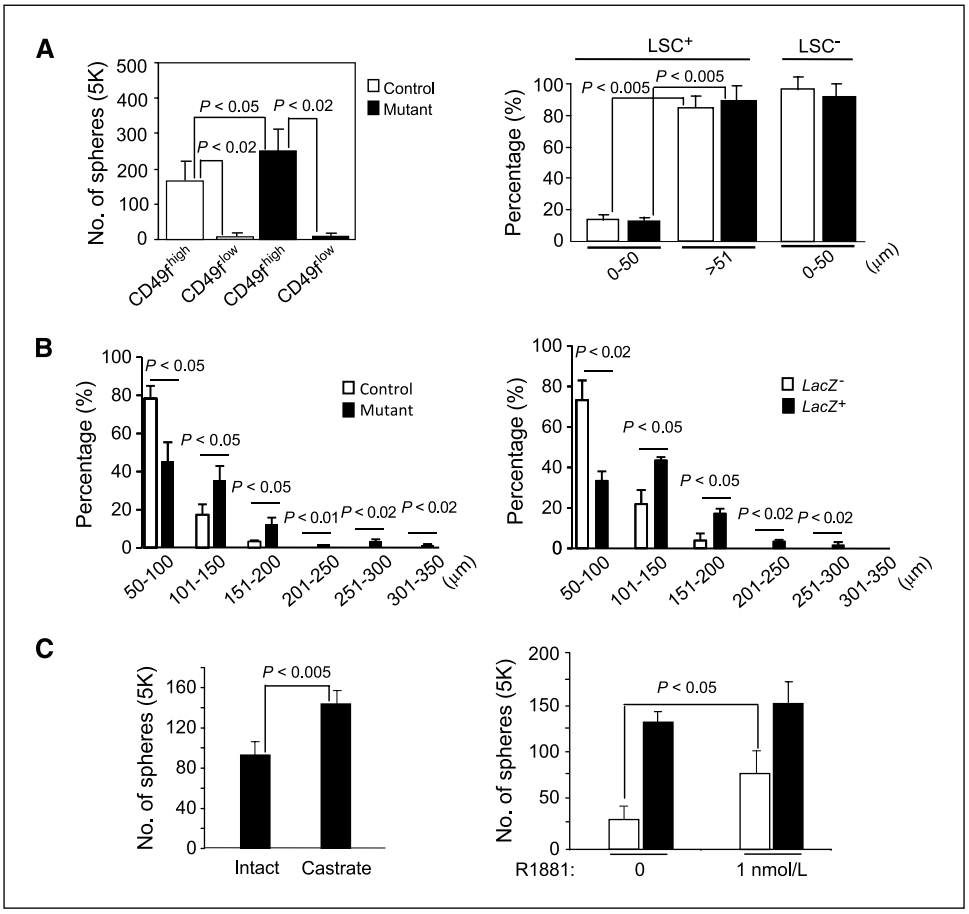

Figure 2. Prostate spheres derived from *Pten* mutants are larger and more heterogeneous than *control* spheres. *A,* CD49f^{high} cells isolated from *Pten* mutant mice contain the most sphere-forming activity ($n = 3$). Whereas LSC$^+$ cells formed spheres that were predominantly >50 μm in diameter, LSC$^-$ cells formed small, nonspheroid structures that were exclusively <50 μm in diameter (*right*). *B,* prostate spheres formed from *ROSA26-LacZ;Pb-Cre$^+$;Pten$^{L/L}$* mice provide genetic validation that *Pten* deletion (LacZ$^+$) leads to enhanced sphere diameter compared with *WT* (LacZ$^-$) spheres. *C,* castration of *Pten* mutant mice enhances sphere-forming potential ($P < 0.005$); however, exogenous androgen (R1881) supplement to mutant sphere cultures from intact mice does not significantly enhance sphere-forming activity ($P > 0.05$).

Results

Relative abundance of LSC subpopulation correlates with progression in the *Pten* mutant prostate cancer model. Previously, we have shown that the LSC subpopulation carries prostate stem/progenitor cell activity in *WT* murine prostate (4). To test the functional significance of the LSC subpopulation in the etiology of prostate cancer, we set out to first determine the relative abundance of these cells in the *Pb-Cre$^+$;Pten$^{L/L}$* prostate cancer model using age-matched and genetic background–matched *Pb-Cre$^-$;Pten$^{L/L}$* mice as controls. *Pb-Cre$^+$;Pten$^{L/L}$* and *Pb-Cre$^-$;Pten$^{L/L}$* mice are herein to be called mutant and control mice, respectively.

Pten mutant mice develop prostate cancer with well-defined kinetics: hyperplasia at 4 weeks, prostate intraepithelial neoplasia at 6 weeks, and invasive adenocarcinoma at 9 weeks (14). Given this, we considered whether disease progression could associate with the relative LSC content by evaluating the mutant prostate at prostate intraepithelial neoplasia (7 weeks) and advanced cancer (20 weeks) stages with age-matched and genetic background–matched controls. Consistent with our previous study (4), we were able to detect 4 ± 0.41% LSC$^+$ cells in controls at age 7 weeks and 4 ± 0.8% LSC$^+$ cells at age 20 weeks. On the other hand, we observed 1.6-fold ($P < 0.002$) and 3.3-fold ($P < 0.0005$) more LSC$^+$ cells at prostate intraepithelial neoplasia (6.5 ± 0.75%) and cancer (13 ± 1.91%) stages in the mutant prostates (Fig. 1*A*). Therefore, LSC$^+$ cell content correlates with disease progression in the *Pten*-null prostate cancer model.

Similar to majority of human prostate cancers, *Pten* mutant prostate glands do respond to androgen ablation, as indicated by increased cell death and reduced gross size, but are able to regrow after prolonged castration (14). Therefore, we asked whether repopulation of prostatic epithelium in surgically castrated mice is correlated with enhanced stem/progenitor cell content. Age-matched and genetic background–matched control and mutant mice were either castrated or left intact at 6 weeks and then analyzed for LSC content at age 10 weeks, the time point when we observed castrate-resistant prostate cancer.[5] Castration of mice at 6 weeks and evaluation for LSC content at 10 weeks indicated a significant increase in the LSC$^+$ subpopulation in both control (Fig. 1*B, open columns*; $P < 0.005$) and mutant (Fig. 1*B, filled columns*; $P < 0.002$) prostates. This suggested that androgen ablation may enhance the percentage of LSC subpopulation in both control and mutant prostates.

Our previous study showed that *Pten* deletion leads to expansion of a subset of prostate cancer cells positive for the basal epithelial markers such as CK5 and p63 (15), similar to the markers used to identify the LSC subpopulation by FACS analysis (4, 7). We then considered whether enhanced LSC content would correlate with these lineage marker-positive cells (15). Immunohistochemistry analyses showed that castration leads to a significant increase in p63$^+$ cells in the control prostate, although most of the p63$^+$ cells

[5] Our unpublished observations.

Published OnlineFirst November 3, 2009; DOI: 10.1158/0008-5472.CAN-08-4673

were not proliferative based on the lack of costaining with Ki-67$^+$ (Supplementary Fig. S1, *arrow* in *top left*). In contrast, many of the p63$^+$ cells in castrated, mutant prostates were also Ki-67$^+$, indicating that PTEN loss may promote more prostate stem/progenitor cells to enter cell cycle after castration (Supplementary Fig. S1, *arrows* in *bottom left*), similar to what we have observed in the intact prostate (15). Interestingly, the location of p63$^+$ cells also changes: from basal in the control gland to both basal and luminal in the mutant prostate gland (Supplementary Fig. S1, *left*), suggesting that castration may not only alter the relative content of stem/progenitor cells but also change the microenvironment or niche of the stem/progenitor cells in the *Pten*-null prostate model. Importantly, we validated that CD49f FACS marker can colocalize with CK5$^+$ cytosolic marker near the basement membrane in control prostates (4) and both basal and luminal epithelial compartments in the mutant prostate specimens (Supplementary Fig. S1, *arrowhead* in *right*).

Although the above study shows that CK5$^+$/p63$^+$ basal cells colocalize with CD49f$^+$ cells, a critical marker used in LSC isolation, more quantitative measurement is needed to correlate *in situ* tumor tissue analysis with that of *in vitro* stem/progenitor cells assays. For this, we sorted LSC$^+$ and LSC$^-$ subpopulations from the *WT* and mutant mice, confirmed by PCR genotyping (Supplementary Fig. S2*B*), cytospun onto the glass slides, and costained for p63 and/or CK5 basal and 4′,6-diamidino-2-phenylindole nuclear markers (Fig. 1*C*; Supplementary Fig. S2*A*). p63$^+$/CK5$^+$, p63$^+$/CK5$^-$, or p63$^-$/CK5$^+$ cells were then quantified and presented as the percentages of 4′,6-diamidino-2-phenylindole–positive viable cells within the LSC$^+$ or LSC$^-$ subpopulation. More than 80% of the *WT* (92.0 ± 0.51%) and mutant (84.1 ± 2.5%) LSC$^+$ cells were positive for both p63 and CK5 cytosolic markers. In contrast, <11% of *WT* (2.8 ± 0.16%) and mutant (10.5 ± 1.17%) LSC$^-$ cells were p63$^+$/CK5$^+$ (Fig. 1*B*). Interestingly, however, mutant LSC$^-$ cells contained more p63$^+$/CK5$^+$ cells than *WT* LSC$^-$ cells at a statistically, significant level. This quantitative analysis gives us confidence that we can directly correlate our *in situ* pathohistologic analysis to LSC-mediated stem/progenitor cell studies.

***Pten* mutant prostate spheres are larger and more heterogeneous than control spheres.** Our previous analysis suggests that LSC^{high} and LSC^{low} fractions represent basal and luminal compartments of normal prostate epithelium, respectively (4). We have also shown that the LSC^{high} subpopulation carries greater sphere-forming activity under the defined *in vitro* culture condition (4, 18). We then asked whether the LSC^{high} subpopulation of mutant prostates would carry similar sphere-forming activity as their control counterpart. As shown in Fig. 2*A*, LSC^{high} cells isolated possess the majority of sphere-forming activities ($P < 0.005$) defined as sphere diameter >50 μm for both control (84.5 ± 7.7%) and mutant (86.5 ± 8.2%) cells (ref. 19; Fig. 2*A, left*). Conversely, the majority of LSC^{low} cells formed structures of <50 μm (Fig. 2*A*,

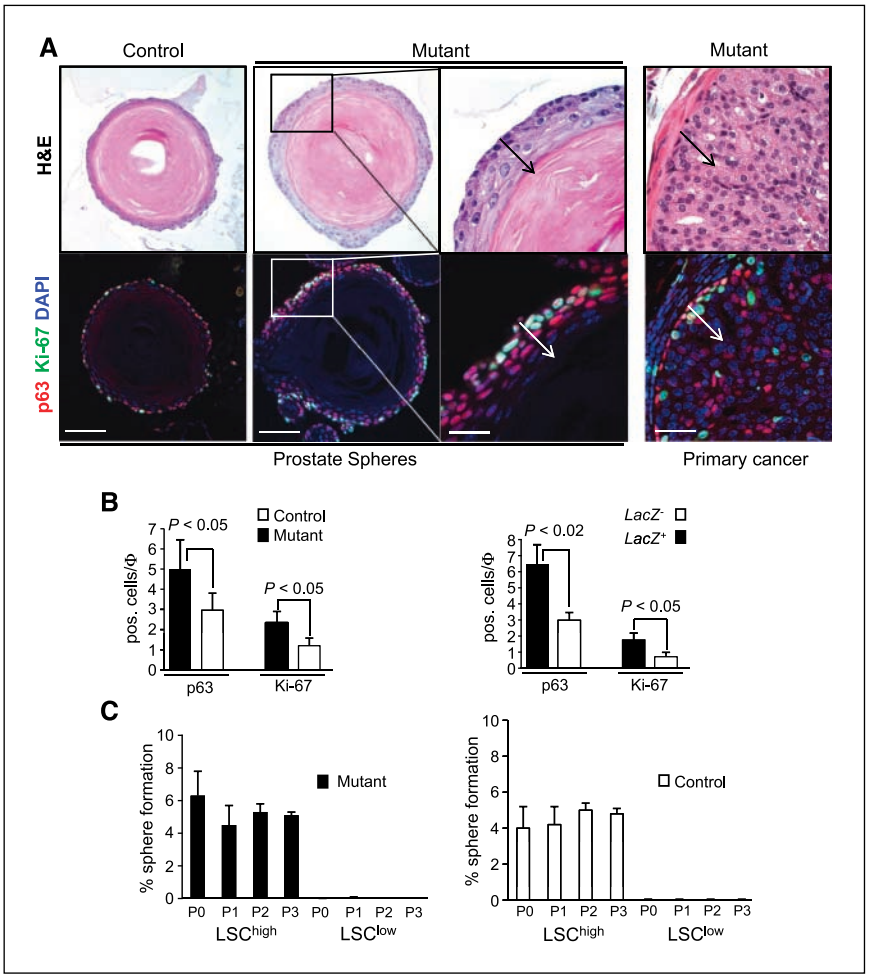

Figure 3. Deletion of *Pten* promotes progenitor expansion in prostate spheres. *A*, immunocytochemical analysis showing that mutant spheres (*middle two*) have a multilayered structure with increased p63$^+$ and Ki-67$^+$ cells, similar to the primary cancer (*right*). *Bar,* 100 μm (*left* and *middle*), 40 μm (*inset*), and 75 μm (*right*). *B, Pten*-null spheres (LacZ$^+$) display progenitor expansion and increased cell proliferation index (*right*). Similar trends can also be observed in the absence of the LacZ marker in spheres generated from total unsorted cells (*left*). *C,* spheres from sorted LSC^{high} cells can be serially passed. Conversely, LSC^{low} fractions yielded very inefficient sphere-forming activities for both control and mutant cultures and could not be serial passaged.

Published OnlineFirst November 3, 2009; DOI: 10.1158/0008-5472.CAN-08-4673

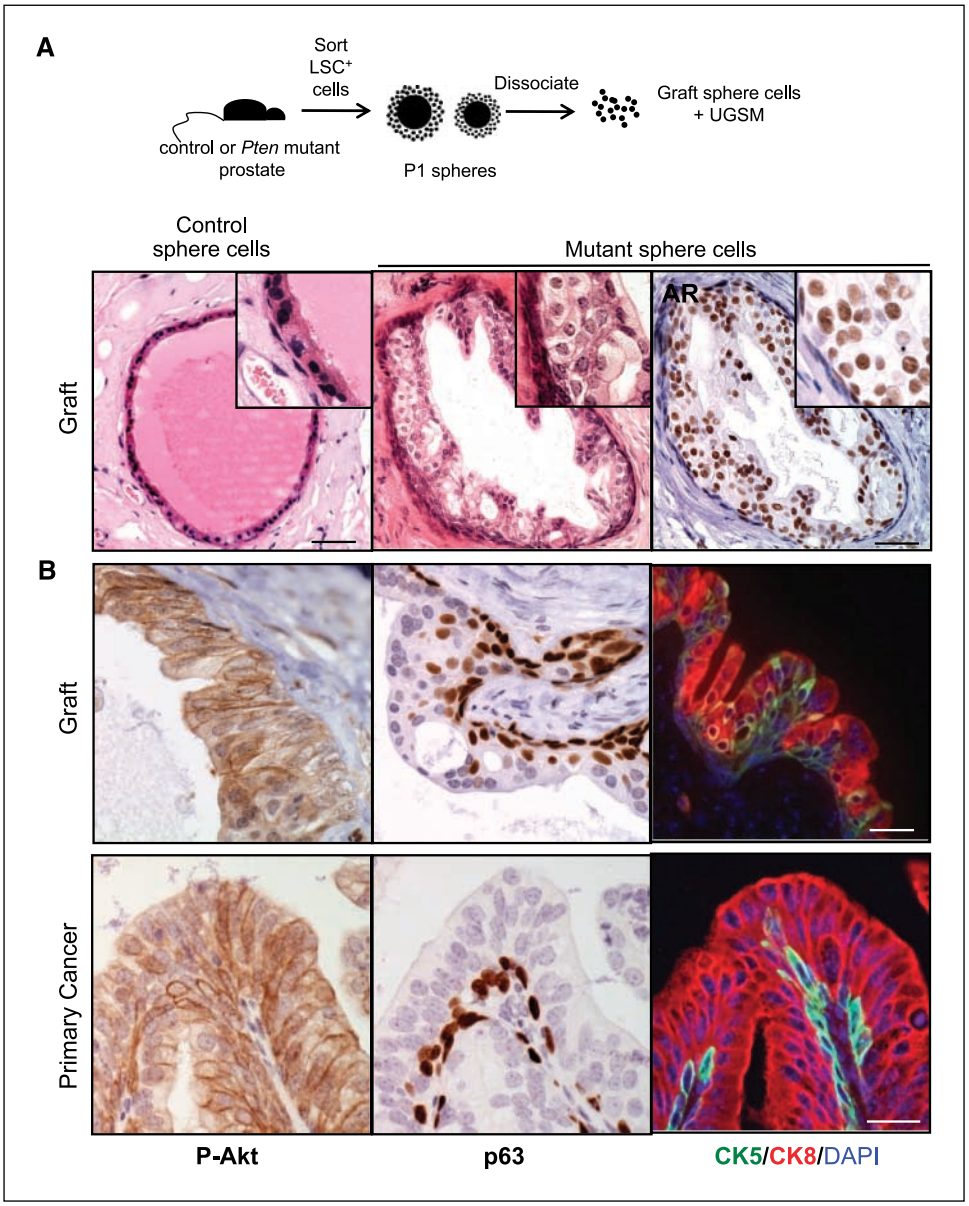

Figure 4. Cells derived from mutant spheres are capable of generating cancerous structure upon *in vivo* reconstitution. *A, top,* a schematic illustration of experimental procedure. LSC cells from either control or *Pten* mutant prostates (6-8 wk) were plated in sphere-forming conditions, expanded by one passage (P_1), dissociated to single cells, and combined with cells from UGSM in Matrigel/prostate epithelial growth medium for grafting. Whereas cells from control spheres formed single-layered prostate acini, sphere cells from mutant mice propagated multilayered AR^+ neoplastic structures (*bottom*). *Bar,* 75 μm. *B,* grafts generated from mutant spheres (*top*) recapitulate phenotypes associated with primary cancer (*bottom*), including expansion of $p63^+/CK5^+$ cells and activation of the PTEN downstream effector P-AKT. *Bar,* 50 μm.

right). Interestingly, when age-matched and genetic background–matched control and mutant prostates were compared, we observed ~1.5-fold ($P < 0.05$) higher sphere-forming activity in the mutant LSC^{high} cells (Fig. 2*A, left*).

Morphologic comparison indicates that spheres derived from the mutants affirm greater size distribution and heterogeneity when compared with spheres propagated from the control prostatic epithelium (Fig. 2*B, left*; Supplementary Fig. S3*A*). Whereas most control spheres consisted of double-layered or "canalized" spheres, mutant spheres vary in size and morphology (Supplementary Fig. S3*A*; data not shown). Prostate spheres derived from the mutants (ages 6-8 weeks) were also statistically bigger, residing more frequently in larger diameter categories ($P < 0.05$ for 101-150 and 151-200 μm and $P < 0.02$ for 251-300 and 301-350 μm), similar to our previous observations of *Pten*-null neurospheres (20, 21). To further validate that PTEN intrinsically controls sphere size, we took the advantage of incomplete *Pten* deletion in 2- to 4-week-old prostate due to different levels of Cre expression in various prostate lobes (14, 22). By crossing *ROSA26-LacZ* reporter mice (16) with *Pb-Cre*$^+$;*Pten*$^{L/L}$ mice, we used *LacZ*$^+$, as measured by X-gal staining, to mark *Pten*-null cells in our sphere culture assay as both *LacZ* reporter activation and *Pten* gene deletion are controlled by the same *Cre* transgene (Supplementary Fig. S3*B*). Under clonal plating conditions (18), the number and size of *LacZ*$^+$ and *LacZ*$^-$ spheres can be accurately measured within the same culture dish. Using this approach, we validated that PTEN intrinsically controls prostate sphere size (Fig. 2*B, right*). The majority of $LacZ^-$ *WT* spheres were found to be within the 50 to 100 μm diameter range, whereas $LacZ^+$ *Pten*-null spheres were found to be distributed in higher numbers throughout the 50 to 200 μm ranges (Fig. 2*B, right*). To validate that prostate spheres did not arise from cells that carry heterozygous *Pten* deletion, we isolated individual spheres and conducted PCR genotype analysis (Supplementary Fig. S4*A*), similar to our previous study of neurospheres (21). Of 30 spheres analyzed, 26 of 30 carried homozygous deletion of floxed *Pten* exon 5 alleles as indicated by the Δ5 band and concordant loss

Published OnlineFirst November 3, 2009; DOI: 10.1158/0008-5472.CAN-08-4673

of the loxp band. The remaining four spheres showed the floxed *Pten* band. No spheres analyzed were *Pten* heterozygous.

Similar to our quantitative LSC measurements, we observed enhanced sphere-forming activity when the mutants were castrated (Fig. 2*C, left*; $P < 0.005$), further supporting that *in vivo* LSC content, as measured by FACS analysis (Supplementary Fig. S1*A*), is related to *in vitro* sphere-forming potential. Interestingly, addition of androgen (1 nmol/L R1881) led to increased sphere number in the control culture ($P < 0.05$) but had little influence on the mutant sphere number obtained from intact mice ($P > 0.05$), consistent with the notion that PTEN can control $p63^+$ basal stem/progenitor cell proliferation in the absence of androgen (Fig. 2*C, right*; Supplementary Fig. S1*B*).

Deletion of *Pten* promotes progenitor expansion in prostate spheres. The finding that mutant LSC^{high} cells formed larger spheres than their control counterparts suggests that *Pten* deletion may lead to the formation of spheres with an increased content of proliferating cells, similar to *Pten*-null neurospheres (21). To explore this hypothesis, we carried out immunohistochemical analysis on individual spheres propagated from control and *Pten* mutant prostates (Fig. 3*A*). Whereas control spheres were typically composed of a single layer of $p63^+$ basal epithelium with limited proliferative activity (Fig. 3*A, left*), mutant spheres showed marked expansion of $p63^+$ cells (Fig. 3*A, middle*), similar to the primary cancer (Fig. 3*A, right*). When costained with Ki-67, a cell proliferation marker, we found that the majority of $Ki\text{-}67^+$ cells in the mutant spheres were also $p63^+$. These data indicate that mutant spheres recapitulate phenotypes associated with the basal compartment of primary cancer in *Pten* mutant prostate. To support this observation using a more quantitative assay, we then analyzed the number of $p63^+$ and $Ki\text{-}67^+$ cells per sphere, normalized by sphere diameter (Ô). Quantitative analysis of P_0 cultures generated from total cells of *ROSA26-LacZ;Pb-Cre*$^+$*;Pten*$^{L/L}$ prostates indicated 1.7- and 1.9-fold enhancements for $p63^+$ ($P < 0.05$) and $Ki\text{-}67^+$ ($P < 0.05$) index, respectively, in mutant spheres (*left*). Similarly, 2.2- and 2.4-fold increases in $p63^+$ ($P < 0.02$) and $Ki\text{-}67^+$ ($P < 0.05$) cells, respectively, was observed in $LacZ^+$ spheres compared with $LacZ^-$ spheres (Fig. 3*B, right*). Of total spheres counted in this assay, 15.2 ± 4.2% were observed to be $LacZ^-$. Thus, mutant spheres contained more $p63^+$ and $Ki\text{-}67^+$ cells than control spheres. Because

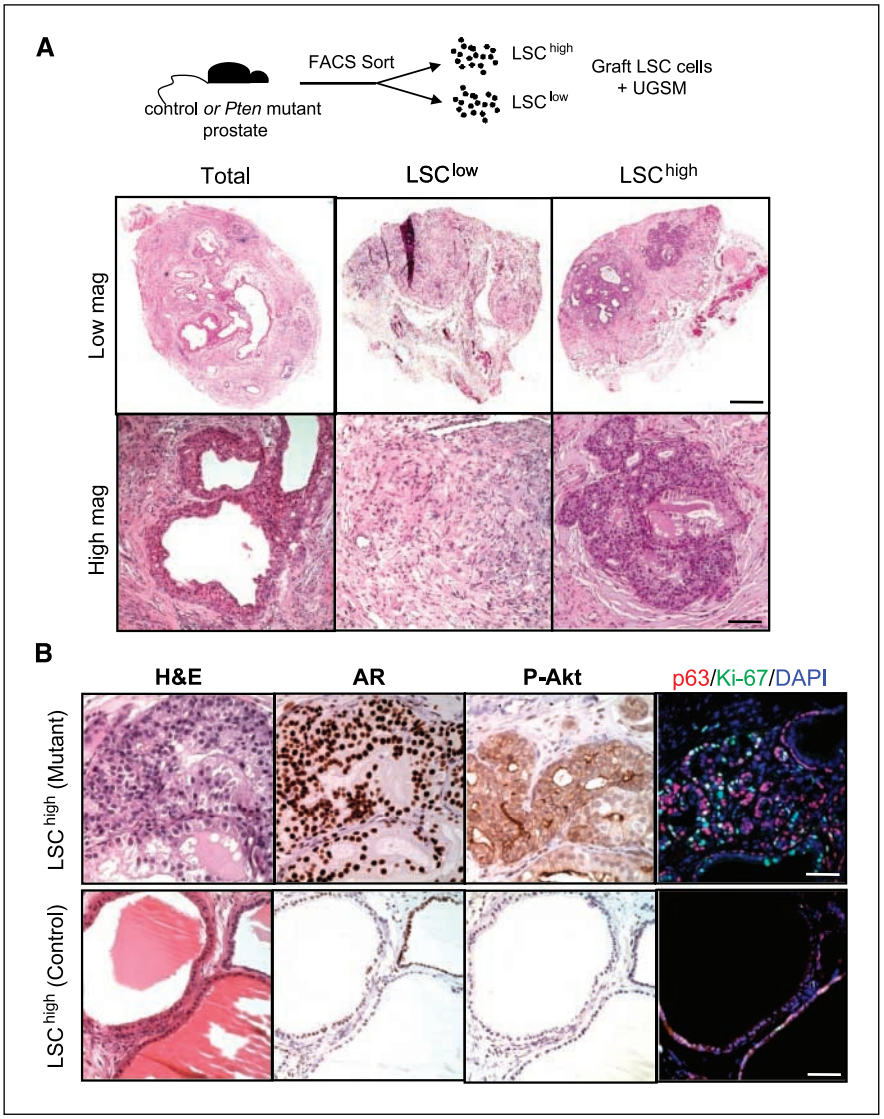

Figure 5. LSC cells from *Pten* mutant mice can initiate prostate cancer development. *A,* total (Lin^-), LSC^{low}, or LSC^{high} sorted cells from *Pten* mutant prostates (6-8 weeks) were each recombined with UGSM cells. Tissue regenerations revealed that whereas total and LSC^{high} cells could reconstitute prostate cancer structure, LSC^{low} cells generated little detectable glandular structure. *Bar,* 500 μm (low magnification) and 200 μm (high magnification). *B,* prostate regenerations from mutant LSC^{high} cells recapitulate primary cancer morphology with AR^+ and $P\text{-}AKT^+$ cells in addition to increased $p63^+$ and $Ki\text{-}67^+$ index (*top*). Control LSC^{high} grafts mimic primary normal prostate structure containing low levels of P-AKT and $p63^+$ cells (*bottom*). *Bar,* 100 μm.

Published OnlineFirst November 3, 2009; DOI: 10.1158/0008-5472.CAN-08-4673

prostate spheres are clonally derived (Supplementary Fig. S5), these data suggest that *Pten*-null sphere cells have a higher proliferative index than control sphere cells.

Our previous studies also indicate that *WT* spheres derived from the LSC^+ subpopulation can be serially passaged, a measurement for stem/progenitor self-renewal capacity, and those LSC^- cells cannot (18). Thus, we asked whether *Pten* loss leads to any change in the self-renewal capacity of its stem/progenitor cells. Plating LSC^{high} control and mutant cells resulted in 3.3% to 5.0% and 4.0% to 8.0% sphere-forming activities during P_0-P_3 passaging, respectively. Conversely, LSC^{low} fractions yielded inefficient sphere-forming activities in both control and mutant cultures. Moreover, LSC^{low} subpopulation could not be serial passaged (Fig. 3*C*).

Cells derived from *Pten* mutant spheres can recapitulate *in vivo* primary cancer morphology. We then asked whether sphere cells derived from mutants were capable of tissue regeneration and propagating an *in vivo* cancer phenotype akin to the *Pten* prostate cancer model. For this, control and mutant LSC^{high} sorted epithelial cells, from mice ages 6 to 8 weeks, were expanded to first passage (P_1) spheres. Spheres were then dissociated to single cells and grafted s.c. in combination with E16/17 UGSM (ref. 18; Fig. 4*A, top*). Each graft consisted of 4×10^3 sphere-dissociated cells and 1×10^5 UGSM cells, mixed in Matrigel/prostate epithelial growth medium and injected s.c. on the dorsal flank of a SCID mouse. After 8 weeks, examination of grafts by a pathologist, derived from control prostate spheres, revealed prostatic acini lined by a single epithelial layer, a phenotype consistent with normal prostatic structure (Fig. 4*A, left*). Grafts derived from mutant spheres, however, generated multilayered AR^+ abnormal structures (Fig. 4*A, right*), similar to phenotypes observed in primary *Pten*-null prostate (Fig. 4*B, bottom*). Significant expansion of cells positive for progenitor markers (p63/CK5) was also observed in mutant sphere grafts in conjunction with activated phosphoinositide 3-kinase signaling as measured by $P\text{-}AKT^{S473}$ (Fig. 4*B, top*). Moreover, increased cell proliferation, which was observed in the mutant spheres, was also preserved in the sphere cell–derived grafts in comparison with control sphere grafts ($13 \pm 4\%$ Ki-67^+ for mutant and 1% Ki-67^+ for control; $P < 0.05$). The observed p63 expansion and activated phosphoinositide 3-kinase signaling effectors in mutant grafts are also consistent with the phenotypes observed in primary tumors (Fig. 4*B, bottom*).

LSC^{high} subpopulation from *Pten* mutants is both necessary and sufficient to initiate tumorigenesis *in vivo*. Because cells derived from *Pten* mutant prostate spheres are capable of regenerating cancerous glandular structures, we then investigated whether the LSC cells that form spheres are the cells-of-origin for cancer in the *Pten*-null mouse model. To do this, we compared total, LSC^{high}, and LSC^{low} cells from intact mutant prostates at ages 6 to 8 weeks. Total or sorted subpopulations were combined with *WT* UGSM cells and 50% Matrigel/prostate epithelial growth medium and inoculated s.c. onto SCID mice (Fig. 5*A*). Histologic analysis revealed that grafts with total mutant epithelium generated adenocarcinoma-like structures as determined by a pathologist (Fig. 5*A, left*). Grafts in the LSC^{low} group, on the other hand, were composed predominately of stroma morphology, contributed by the UGSM. Although we could discern small clusters of cells that appear to remain viable, there was little evidence of ductal regeneration and no cancer present. To confirm that the lack of regeneration capacity in LSC^{low} grafts is not due to experiment failure, LSC^{low} mutant cells were mixed with total epithelial cells from *WT* prostate. In this control experiment, the only ductal structure obtained was from *WT* epithelial cells (Supplementary Fig. S6). Importantly, grafts from the LSC^{high} subpopulation yielded cancerous structures (Fig. 5*A, right*) that contained AR^+ cells with activated $P\text{-}AKT^{S473}$ levels, thereby confirming that cells were null for *Pten* activity (Fig. 5*B, top*). *Pten* mutant LSC^{high} cell-derived grafts also showed expansion of Ki-67^+ cells ($15.8 \pm 0.7\%$ Ki-67^+ in mutant grafts versus $2.0 \pm 1\%$ in controls; $P < 0.05$) and $p63^+$ cells compared with grafts derived from control LSC^{high} cells. Collectively, these data show that LSC^{high} cells isolated from *Pten* mutants are sufficient to propagate cancer when subject to *in vivo* regeneration assays, whereas the LSC^{low} subpopulation has significantly less *in vivo* tumorigenic potential.

Discussion

The *Pten* prostate cancer model mimics many aspects of human prostate cancer biology, including the invasive and progressive nature of the disease and the alteration of disease relevant gene expression (14, 15, 23). In this study, we showed that the majority of cancer-initiating activity is contained within the LSC^{high} subpopulation within *Pten*-null epithelium. Our study validated that structural and functional differences between normal and *Pten*-null prostate glands can be recapitulated within the LSC subpopulation by *in vitro* sphere culture and *in vivo* regeneration assays using cells derived from either sphere culture or freshly isolated from primary cancers. An important finding from our study is that the basal-like cells, as defined by LSC FACS analysis, of *Pten*-null prostate cancer model contains the majority of tumor-initiating function, whereas the more differentiated luminal component has very little such activity. The lack of tumor-initiating activity of mutant LSC^{low} subpopulation is likely attributed to the lack of progenitor/stem cells, similar to the *WT* LSC^{low} subpopulation (4). Consistent with our previous study that p63 and CK5 basal cell markers are separated in a minor population of cells within or immediately above the basal compartment of the *Pten*-null prostate gland (23), we observed more LSC^+ cells from the mutant that are negative for p63/CK5 than its *WT* counterpart (10.3% versus 2.6%), suggesting that *Pten* deletion may lead to the expansion of the potential intermediate or transit amplifying cells, which may also be capable of cancer initiation. Moreover, it is possible that not all cells within LSC^+ pool have the same potential for cancer initiation. It is clear, however, that the majority of normal and oncogenic progenitor function is contained within the LSC^+ population as defined by the LSC immunophenotype.

The capacity of $CD49f^{high}$ to enrich for basal subpopulations is not restricted to prostate but has also been shown in skin (24) and mammary epithelium (25). For example, using mammary fat pad transplantation assays, $CD49f^{high}$ and $CD49f^{low}$ subpopulations were shown to be critical in determining the presence or absence of progenitor function, respectively (25). Interestingly, gene expression analysis showed CD49f to be highly expressed in tumor-initiating $CD44^+/CD24^-$ subpopulation (26), supporting the potential role of $CD49f^+$ cells in human mammary gland carcinogenesis.

Although we have shown that the LSC^{high} subpopulation contains cells with the capacity for regeneration of an oncogenic phenotype, there are several important questions that remain to be answered. Is a single cell from the $Lin^-Sca\text{-}1^+CD49f^{high}$ subpopulation capable of multilineage differentiation and reconstituting a normal prostate or tumorigenic prostate? Are such reconstituted oncogenic structures capable of serial transplantation and therefore have the ability of self-renewal? Several studies of this type have been carried out using *WT* cells, including the mammary

Published OnlineFirst November 3, 2009; DOI: 10.1158/0008-5472.CAN-08-4673

gland (27) and murine prostate (6). Using a single cell from the $Lin^-CD29^{high}CD24^+$ subpopulation, an entire mammary gland with normal function was regenerated (27). As a corollary, it is interesting that $Lin^-CD29^{high}CD24^+$ subpopulation is also significantly increased in the MMTV-Wnt1 breast cancer model, thereby implying a functional interaction between Wnt signaling and mammary stem cells (27). It has also been reported that a single cell from the $Lin^-Sca\text{-}1^+CD133^+CD44^+CD117^+$ subpopulation can generate *WT* prostatic acini, which can be antagonized using an anti-CD117 monoclonal antibody (6). Whether a single cancer stem cell can reconstitute oncogenic structure has yet to be determined.

That the LSC population contains the majority of sphere and regenerative potential provides motivation for targeted therapy of cancer initiation in murine prostate cancer models. Moreover, it is conceivable that in human disease antiandrogen therapy selects for subpopulations of oncogenic progenitor cells with "stemness" qualities similar to those found in the LSC subpopulation. Although it is tempting to directly extrapolate findings from mice to humans, it is important to consider critical anatomic, biological, and marker expression differences between these systems. To date, few surface markers have been shown to be functionally relevant to both mouse and human prostate cancer-initiating cells. Thus, to more accurately bridge findings obtained using murine cancer models to that of human disease, it will be important to consider how progenitor cell expansion in the basal compartment in the murine prostate may relate to human disease, in which the cell-of-origin for resistant disease may occur by clonal expansion and/or derivation from a particular or multiple cell compartments. Thus, common cell surface markers that can be used to identify the tumor-initiating subpopulations from mouse and humans prostate cancers will be critical.

Disclosure of Potential Conflicts of Interest

No potential conflicts of interest were disclosed.

Acknowledgments

Received 12/11/08; revised 8/21/09; accepted 9/15/09; published OnlineFirst 11/3/09.

Grant support: NIH grants F32 CA112988-01 (D.J. Mulholland), K99CA125937 (L. Xin), and R01 CA107166 and RO1 CA121110 (H. Wu) and Prostate Cancer Foundation (D. Lawson, H. Wu, and O. Witte).

The costs of publication of this article were defrayed in part by the payment of page charges. This article must therefore be hereby marked *advertisement* in accordance with 18 U.S.C. Section 1734 solely to indicate this fact.

We thank our colleagues in our laboratories for helpful comments and suggestions.

References

1. Gronberg H. Prostate cancer epidemiology. Lancet 2003;361:859–64.
2. English HF, Santen RJ, Isaacs JT. Response of glandular versus basal rat ventral prostatic epithelial cells to androgen withdrawal and replacement. Prostate 1987; 11:229–42.
3. Isaacs J. Washington (DC): U.S. Department of Health and Human Services; 1985.
4. Lawson DA, Xin L, Lukacs RU, Cheng D, Witte ON. Isolation and functional characterization of murine prostate stem cells. Proc Natl Acad Sci U S A 2007; 104:181–6.
5. Bonkhoff H. Neuroendocrine differentiation in human prostate cancer. Morphogenesis, proliferation and androgen receptor status. Ann Oncol 2001;12 Suppl 2:S141–4.
6. Leong KG, Wang BE, Johnson L, Gao WQ. Generation of a prostate from a single adult stem cell. Nature 2008;456:804–8.
7. Xin L, Lawson DA, Witte ON. The Sca-1 cell surface marker enriches for a prostate-regenerating cell subpopulation that can initiate prostate tumorigenesis. Proc Natl Acad Sci U S A 2005;102:6942–7.
8. Goldstein AS, Lawson DA, Cheng D, Sun W, Garraway IP, Witte ON. Trop2 identifies a subpopulation of murine and human prostate basal cells with stem cell characteristics. Proc Natl Acad Sci U S A 2008;105:20882–7.
9. Patrawala L, Calhoun-Davis T, Schneider-Broussard R, Tang DG. Hierarchical organization of prostate cancer cells in xenograft tumors: the $CD44^+\alpha_2\beta_1^+$ cell population is enriched in tumor-initiating cells. Cancer Res 2007;67:6796–805.
10. Collins AT, Berry PA, Hyde C, Stower MJ, Maitland NJ. Prospective identification of tumorigenic prostate cancer stem cells. Cancer Res 2005;65:10946–51.
11. Miki J, Rhim JS. Prostate cell cultures as *in vitro* models for the study of normal stem cells and cancer stem cells. Prostate Cancer Prostatic Dis 2008;11:32–9.
12. Vander Griend DJ, Karthaus WL, Dalrymple S, Meeker A, Demarzo AM, Isaacs JT. The role of CD133 in normal human prostate stem cells and malignant cancer-initiating cells. Cancer Res 2008;68:9703–11.
13. Suzuki A, Nakano T, Mak TW, Sasaki T. Portrait of PTEN: messages from mutant mice. Cancer Sci 2008; 99:209–13.
14. Wang S, Gao J, Lei Q, et al. Prostate-specific deletion of the murine Pten tumor suppressor gene leads to metastatic prostate cancer. Cancer Cell 2003;4:209–21.
15. Wang S, Garcia AJ, Wu M, Lawson DA, Witte ON, Wu H. Pten deletion leads to the expansion of a prostatic stem/progenitor cell subpopulation and tumor initiation. Proc Natl Acad Sci U S A 2006;103:1480–5.
16. Soriano P. Generalized lacZ expression with the ROSA26 Cre reporter strain. Nat Genet 1999;21:70–1.
17. Xin L, Ide H, Kim Y, Dubey P, Witte ON. *In vivo* regeneration of murine prostate from dissociated cell populations of postnatal epithelia and urogenital sinus mesenchyme. Proc Natl Acad Sci U S A 2003;100 Suppl 1:11896–903.
18. Xin L, Lukacs RU, Lawson DA, Cheng D, Witte ON. Self-renewal and multilineage differentiation *in vitro* from murine prostate stem cells. Stem Cells 2007;25:2760–9.
19. Zhigang Z, Wenlu S. Complete androgen ablation suppresses prostate stem cell antigen (PSCA) mRNA expression in human prostate carcinoma. Prostate 2005; 65:299–305.
20. Groszer M, Erickson R, Scripture-Adams DD, et al. PTEN negatively regulates neural stem cell self-renewal by modulating $G_{0\text{-}1}$ cell cycle entry. Proc Natl Acad Sci U S A 2006;103:111–6.
21. Groszer M, Erickson R, Scripture-Adams DD, et al. Negative regulation of neural stem/progenitor cell proliferation by the Pten tumor suppressor gene *in vivo*. Science 2001;294:2186–9.
22. Wu X, Wu J, Huang J, et al. Generation of a prostate epithelial cell-specific Cre transgenic mouse model for tissue-specific gene ablation. Mech Dev 2001; 101:61–9.
23. Lei Q, Jiao J, Xin L, et al. NKX3.1 stabilizes p53, inhibits AKT activation, and blocks prostate cancer initiation caused by PTEN loss. Cancer Cell 2006;9: 367–78.
24. Carter WG, Kaur P, Gil SG, Gahr PJ, Wayner EA. Distinct functions for integrins $\alpha_3\beta_1$ in focal adhesions and $\alpha_6\beta_4$/bullous pemphigoid antigen in a new stable anchoring contact (SAC) of keratinocytes: relation to hemidesmosomes. J Cell Biol 1990;111:3141–54.
25. Stingl J, Eirew P, Ricketson I, et al. Purification and unique properties of mammary epithelial stem cells. Nature 2006;439:993–7.
26. Honeth G, Bendahl PO, Ringner M, et al. The $CD44^+/CD24^-$ phenotype is enriched in basal-like breast tumors. Breast Cancer Res 2008;10:R53.
27. Shackleton M, Vaillant F, Simpson KJ, et al. Generation of a functional mammary gland from a single stem cell. Nature 2006;439:84–8.

Published OnlineFirst November 3, 2009; DOI: 10.1158/0008-5472.CAN-08-4673

Cancer Research
The Journal of Cancer Research (1916–1930) | The American Journal of Cancer (1931–1940)

AACR American Association for Cancer Research

Lin$^-$Sca-1$^+$CD49f^{high} Stem/Progenitors Are Tumor-Initiating Cells in the *Pten*-Null Prostate Cancer Model

David J. Mulholland, Li Xin, Ashkan Morim, et al.

Cancer Res 2009;69:8555-8562. Published OnlineFirst November 3, 2009.